DOI: 10.1002/chem.200600991

A Biomimetic Approach to the Chemical Inactivation of Chrysotile Fibres by Lichen Metabolites

Francesco Turci,[a] Sergio E. Favero-Longo,[b] Maura Tomatis,[a] Gianmario Martra,[a] Daniele Castelli,[c] Rosanna Piervittori,[b] and Bice Fubini*[a]

Abstract: Some lichens were recently reported to modify the surface state of asbestos. Here we report some new insight on the physico-chemical modifications induced by natural chelators (lichen metabolites) on two asbestos samples collected in two different locations. A biomimetic approach was followed by reproducing in the laboratory the weathering effect of lichen metabolites. Norstictic, pulvinic and oxalic acid (0.005, 0.5 and 50 mM) were put in contact with chrysotile fibres, either in pure form (A) or intergrown with balangeroite, an iron-rich asbestiform phase (B). Mg and Si removal, measured by inductively coupled plasma atomic emission spectrometry (ICP-AES) and scanning electron microscopy–energy dispersive X-ray spectroscopy (SEM-EDS), reveals an incongruent dissolution for pure chrysotile (A), with Mg removal always exceeding that of Si, while chrysotile–balangeroite (B) follows a congruent dissolution pattern in all cases except in the presence of 50 mM oxalic acid. A much larger removal of Mg than Si in the solutions of 0.5 and 50 mM oxalic acid with chrysotile (A) suggests a structural collapse, which in the case of chrysotile–balangeroite (B) only occurs with 50 mM oxalic acid; in these cases both samples are converted into amorphous silica (as detected by X-ray diffraction (XRD)). Subsequent to incubation, some new phases (Fe_2O_3, $CaMg(CO_3)_2$, $(C_2O_4)\cdot H_2O$ and $Mg(C_2O_4)\cdot 2H_2O$), similar to those observed in the field, were detected by XRD and micro-Raman spectroscopy. The leaching effect of lichen metabolites also modifies the Fenton activity, a process widely correlated with asbestos pathogenicity: pure chrysotile (A) activity is reduced by 50 mM oxalic acid, while all lichen metabolites reduce the activity of chrysotile–balangeroite (B). The selective removal of poorly coordinated, highly reactive iron ions, evidenced by NO adsorption, accounts for the loss in Fenton activity. Such fibres were chemically close to the ones observed in the field. Chrysotile-rich rocks, colonised by lichens, could be exposed to a natural bioattenuation and considered as a transient environmental hazard.

Keywords: asbestos · iron · lichen metabolites · radicals · surface chemistry

Introduction

Exposure to airborne asbestos fibres causes a severe pneumoconiosis (asbestosis) and malignancies such as bronchogenic carcinoma and pleural mesothelioma.[1–3] Even if the mechanisms of action of asbestos at the molecular level are still partially unclear,[4–6] some physico-chemical features (that is, fibrous habit, high biopersistence, redox-reactive iron ions at the surface) are currently correlated to fibre toxicity.[4,7–9] In spite of its detrimental effects on exposed humans, asbestos is still mined, manufactured and used in various parts of the world and is currently banned only in less than 40 countries.[10] Beside the occupational aspect, asbestos remains an environmental issue everywhere because of disused mines, industrial sites and naturally occurring asbestos outcrops. The decontamination of asbestos fibres dispersed over wide areas of soil obviously requires a different approach from that which is currently proposed for asbestos

[a] Dr. F. Turci, Dr. M. Tomatis, Prof. G. Martra, Prof. B. Fubini
Dipartimento di Chimica IFM, Centre of Excellence of Nanostructured Interfaces and Surfaces (NIS)
and Interdepartmental Centre "G. Scansetti" for Studies on Asbestos and Other Toxic Particulates
University of Torino, via Pietro Giuria 7, 10125 Torino (Italy)
Fax: (+39) 011-670-7577
E-mail: bice.fubini@unito.it

[b] Dr. S. E. Favero-Longo, Prof. R. Piervittori
Dipartimento di Biologia Vegetale, Center of Excellence for Plant and Microbial Biosensing (CEBIOVEM)
and Interdepartmental Centre "G. Scansetti" for Studies on Asbestos and Other Toxic Particulates
University of Torino, viale Mattioli 25, 10125 Torino (Italy)

[c] Prof. D. Castelli
Dipartimento di Scienze Mineralogiche e Petrologiche
and Interdepartmental Centre "G. Scansetti" for Studies on Asbestos and Other Toxic Particulates
University of Torino, via Valperga Caluso 35, 10125 Torino (Italy)

Supporting information for this article is available on the WWW under http://www.chemeurj.org/ or from the author.

localised in buildings. In such cases, the fibres cannot be removed but have to be inactivated in situ, without damaging the environment.

Several studies have shown that natural and synthetic chelators affect asbestos reactivity and pathogenicity.[11–13] The reactivity of iron-rich asbestos is diminished by the action of some organic molecules able to chelate iron (for example, desferrioxamine, ferrozine, green tea catechins, phytic acid).[11,14,15] Such findings evidence the central role of iron in the asbestos-related generation of reactive oxygen species (ROS), a process widely correlated to asbestos pathogenicity.[13] In this context, soil fungi have recently been reported by some of us to modify the chemical composition of asbestos fibres.[16–19]

The symbiotic lichen-forming fungi are well-known physical and chemical weathering agents of natural and artificial mineral substrata.[20,21] Besides the physical effects related to the penetration of fungal hyphae, lichens chemically deteriorate minerals by secreting a wide range of primary and secondary metabolites. Many of these organic substances are characterised by both acidic and chelating functions, which influence the dissolution and precipitation reactions, as well as the neoformation of new mineral phases.[22] Since extracellular metal oxalates were widely detected at the lichen–rock interface, oxalic acid, a primary metabolite secreted by several lichen and other fungal species,[23] is generally recognised as the main actor of chemical weathering processes.[22] Lichen secondary metabolites, the "lichen substances", which comprise aliphatic, cycloaliphatic, aromatic and terpenic compounds,[24,25] may also contribute to the weathering processes, by chelating transition-metal ions.[26–28]

In a previous study, we reported that lichens also degrade chrysotile fibres (serpentine asbestos).[29] Chrysotile $[Mg_3Si_2O_5(OH)_4]$ is composed by the association of a tetrahedral silicate sheet of composition $(Si_2O_5)_n^{2n-}$ with an octahedral brucite sheet of composition $[Mg_3O_2(OH)_4]_n^{2n-}$. The two sheets forming chrysotile fibres are linked to form a 1:1 layered silicate; a slight misfit between the sheets causes curling to form concentric cylinders, with the brucite-like layer on the outside of the cylinder.[30] Iron (generally as Fe^{2+}) substituted for magnesium in the octahedral layer (from 1–6 oxide wt%) and submicroscopic association with accessory minerals (such as tremolite, nemalite, balangeroite) are both considered to modulate the toxicity of chrysotile.[4,9,31–33]

Mg-depleted chrysotile was detected below several lichen species both on natural and anthropogenic substrata, such as chrysotile-bearing rocks and asbestos cement roofs.[29,34] Since oxalates were detected at the lichen–asbestos interface, the chelating action of the oxalic acid secreted by lichens was considered to be mainly responsible for the weathering. Iron, replacing some magnesium in chrysotile, is also extracted during the brucite-layer depletion.

The aim of the present study is to analyse the variation in chemical properties involved in the toxicity[4,35,36] of the lichen-modified fibres.

A biomimetic approach was followed by reproducing in the laboratory the weathering effects of lichen metabolites on chrysotile fibres, as previously observed in nature.[29] Two chrysotile specimens, pure (A) or intergrown (B) with an iron-rich asbestiform phase (balangeroite), have been studied. Three lichen metabolites differing in their chemical nature have been used, namely oxalic acid (a primary metabolite, **1**), norstictic acid and pulvinic acid (secondary metabolites and aromatic esters, **2** and **3**). In the case of oxalic acid, a wide range of concentrations (0.005–50 mM) was used. The analyses have been focussed on:

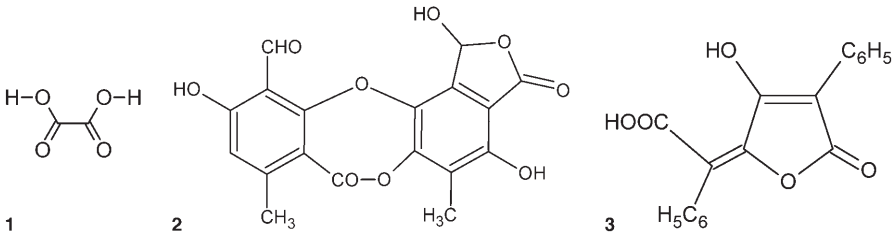

1) Evaluation of ion release during incubation with lichen-metabolite solutions and consequent transformation of the chrysotile structure.
2) Variation in the coordinative state of iron at the surface of the fibres.
3) Modification of the potential of the fibres to release free radicals.

Results

Modification induced in the bulk: leaching processes

Atomic emission spectroscopy (ICP-AES): The concentrations of silicon and magnesium were measured in the supernatant of pure chrysotile and chrysotile–balangeroite filtrates and are shown in Figure 1A and B, respectively. The iron concentration is not reported because of the competing effect of precipitation of iron hydroxides ($K_{sp} = 1.1 \times 10^{-36}$; K_{sp} = solubility product) that occurs at the working pH value of some of the solutions. The two fibres exhibit quite a different behaviour. It is noteworthy that the leaching of magnesium from pure chrysotile greatly exceeds that of silicon in all cases. By contrast, the same amount of magnesium and silicon is released from the chrysotile–balangeroite, with the only exception being the 50 mM oxalic acid solution.

Pure chrysotile (A): Water, secondary metabolites and 0.005 mM oxalic acid determine a slight solubilisation of

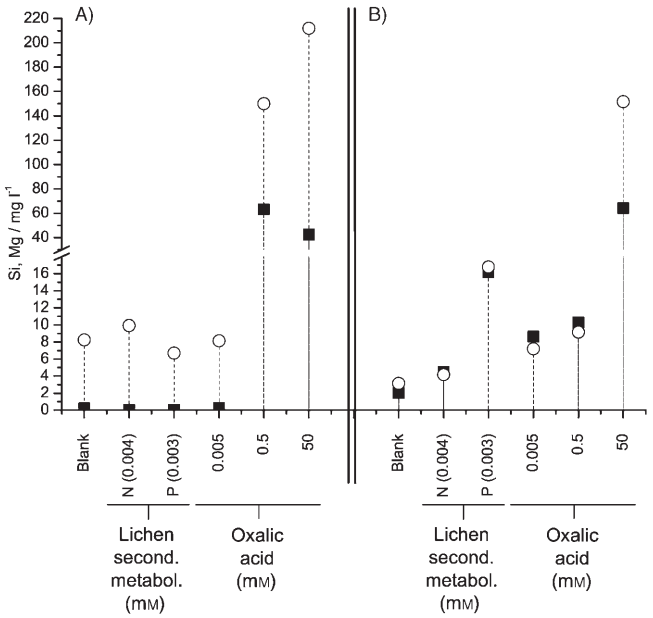

Figure 1. Concentration of silicon (■) and magnesium (○) measured with ICP-AES in the supernatant of suspensions of chrysotile fibres (A) and chrysotile–balangeroite fibres (B) after incubation with deionised water (blank), norstictic acid (N), pulvinic acid (P) or oxalic acid solutions for 35 d in the dark. As the result of ICP-AES describes an average process concerning a relatively large amount of mineral fibres, a single analysis was performed on the supernatant obtained from a representative amount of the starting material.

magnesium (approximately 8 mg L^{-1}), while no silicon is detected under the same conditions. Concentrations of 0.5 and 50 mM of oxalic acid drastically remove both magnesium and silicon from the mineral structure. Noticeably, the amounts of magnesium leached after incubation with 0.5 and 50 mM oxalic acid rise to 59 (149 mg L^{-1}) and 84% (212 mg L^{-1}), respectively, of the total magnesium content of this specimen (252 mg L^{-1}).

Chrysotile–balangeroite (B): The cation concentration in the supernatant depends on the leaching contributions of both the chrysotile and balangeroite phases. Norstictic acid, pulvinic acid and 0.005 and 0.5 mM oxalic acid determine a slight release of both magnesium and silicon into the supernatant. In particular, pulvinic acid exhibits a higher effect (Si = 16 and Mg = 17 mg L^{-1}) than the other lichen metabolites. Only 50 mM oxalic acid yields a deeper leaching of the sample, up to 64 and 152 mg L^{-1} of silicon and magnesium, respectively.

Scanning electron microscopy (SEM): The two original fibres, incubated in water (blank), exhibit a remarkably different morphology (Figure 2A and C). Fibres of both samples leached with 0.005 and 0.5 mM oxalic acid and with secondary metabolites did not show any detectable morphologic modification following incubation (data not shown). Substantial alterations are, however, observed after incubation with 50 mM oxalic acid (Figure 2B and D).

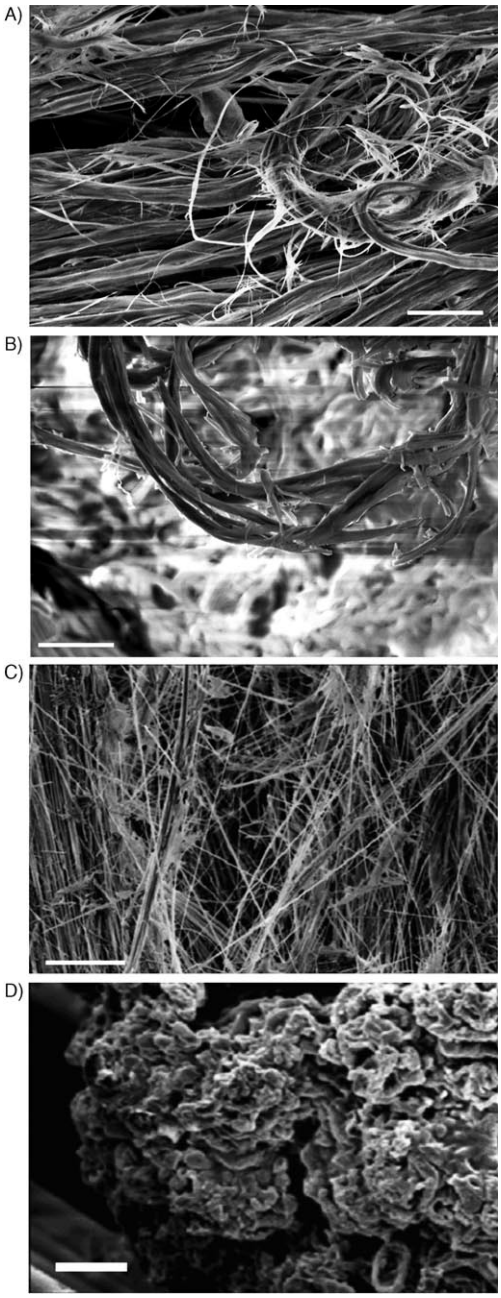

Figure 2. Solid residuals of pure chrysotile (A, B) and chrysotile–balangeroite (C, D) after the incubation with water (A, C) or 50 mM oxalic acid (B, D). Relative scale bars: 20 μm.

Pure chrysotile (A): The chrysotile fibres appear as aggregates of peculiar tubular-shaped fibrils, which are characterised by a long, thin, flexible aspect (Figure 2A). The leaching effect of 50 mM oxalic acid solution (Figure 2B) determines a complete solubilisation of the more isolated fibres and yields a sponge-like silica network. Large bundles retain the tubular shape, with a noticeably increased brittleness.

Chrysotile–balangeroite (B): Electron microscopy shows that the fibres of the mixed sample are thinner than the pure chrysotile ones. Occasionally, aggregates of a few fibres are

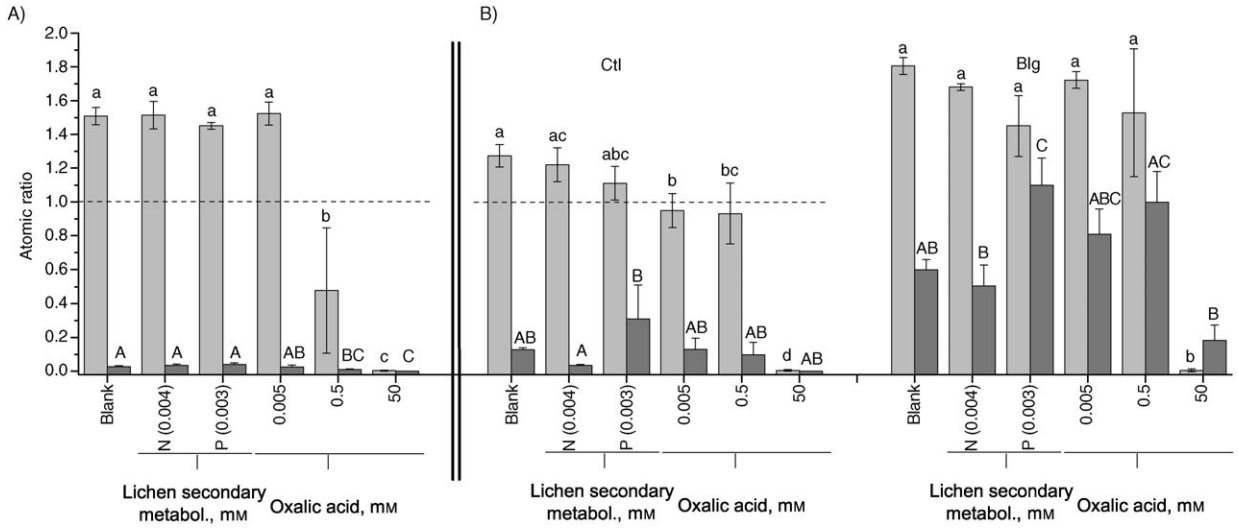

Figure 3. Mg/Si (light grey bars) and Fe/Si (dark grey bars) atomic ratios of pure (A) and mixed (B) fibres incubated with deionised water (blank), norstictic acid (N, approximately 0.004 mM), pulvinic acid (P, approximately 0.003 mM) or oxalic acid (0.005, 0.5 and 50 mM) solutions for 35 d in the dark. A) Data for pure chrysotile. B) Two sets of data, one for the chrysotile phase (Ctl) and one for the balangeroite phase (Blg) of the mixed specimen. ----- represents the Mg/Si atomic ratio of chrysotile colonised by lichens under field conditions (data modified from reference [29]). Atomic ratios are reported as the averages of independent measurements (at least six) ± the standard error. According to Tukey's test (ANOVA), columns which do not share at least one letter are statistically different. Analyses of the solid residuals of the samples, 35 d after the incubation in distilled water, are also reported as blanks.

observed (Figure 2C). The incubation with 50 mM oxalic acid severely modifies the morphology of the fibres, which are converted into a sponge-like Si–O network (Figure 2D).

Energy dispersion spectroscopy (EDS): The elemental analyses of the asbestos fibres before and after incubation with oxalic acid and lichen secondary metabolites (norstictic and pulvinic acid) solutions are reported in Figure 3. In order to correctly represent the weathering dissolution of the two complex asbestos samples, data are expressed as atomic ratios (Mg/Si or Fe/Si). A constant atomic ratio indicates that the dissolution process proceeds congruently with the original stoichiometric composition.[37,38] At least six fibres were analysed for each sample.

Pure chrysotile (A): The chemical composition of the fibre is not significantly modified after treatment with norstictic acid, pulvinic acid or 0.005 mM oxalic acid solution with respect to the sample with pure water. The Mg/Si ratio decreases upon incubation with 0.5 mM oxalic acid solution and the sample shows a wide range of compositions (large error bar), while the Fe/Si ratio is slightly modified. Finally, chrysotile is completely transformed into silica after treatment with 50 mM oxalic acid.

Chrysotile–balangeroite (B): As balangeroite, but not chrysotile, is characterised by the presence of manganese, the two mineral phases can be discriminated on the basis of the Mn peak in the EDS spectra. The brucitic layer of the chrysotile phase (Ctl) is solubilised in all of the incubations performed with oxalic acid, while no modification is observed with norstictic acid and pulvinic acid. The Mg/Si ratio decreases similarly after incubation with 0.005 or 0.5 mM oxalic acid, while magnesium is completely depleted after treatment with 50 mM oxalic acid. The Fe/Si ratio is not significantly affected by any acid. The balangeroite phase (Blg) is only modified after incubation with 50 mM oxalic acid, which determines a significant decrease in the Mg/Si ratio, while remarkably some iron ions remain trapped in the silica structure. Other incubations do not significantly affect the Mg/Si and Fe/Si ratios, although a slight increase in the Fe/Si ratio is observed after the incubation with pulvinic acid.

Noticeably, the compositions of the pure chrysotile after incubation with 0.5 mM oxalic acid and of chrysotile–balangeroite treated with 0.005 and 0.5 mM oxalic acid are similar to that detected below lichens under field conditions.[29]

Structural modification and precipitation of neo-formed compounds: The X-ray diffraction patterns of the fibres are reported in Figure 4. Pure chrysotile (A) and chrysotile–balangeroite (B) keep their crystallinity after treatment with 0.005 and 0.5 mM oxalic acid and with pulvinic and norstictic acid solutions. In the chrysotile–balangeroite sample (Figure 4B), the contribution of the chrysotile phase to the spectrum profile significantly decreases with respect to balangeroite when the mineral is incubated with the lichen primary and secondary metabolites. Both samples are completely transformed after incubation with the 50 mM oxalic acid solution: an amorphous residual is detected after the leaching of both pure chrysotile (Figure 4A) and chrysotile–balangeroite (Figure 4B). The diffraction pattern of the residuals of this latter sample indicates the formation of some calcium oxalates. The precipitation of calcium oxalate monohydrate, also observed in the field, is related to the occurrence of di-

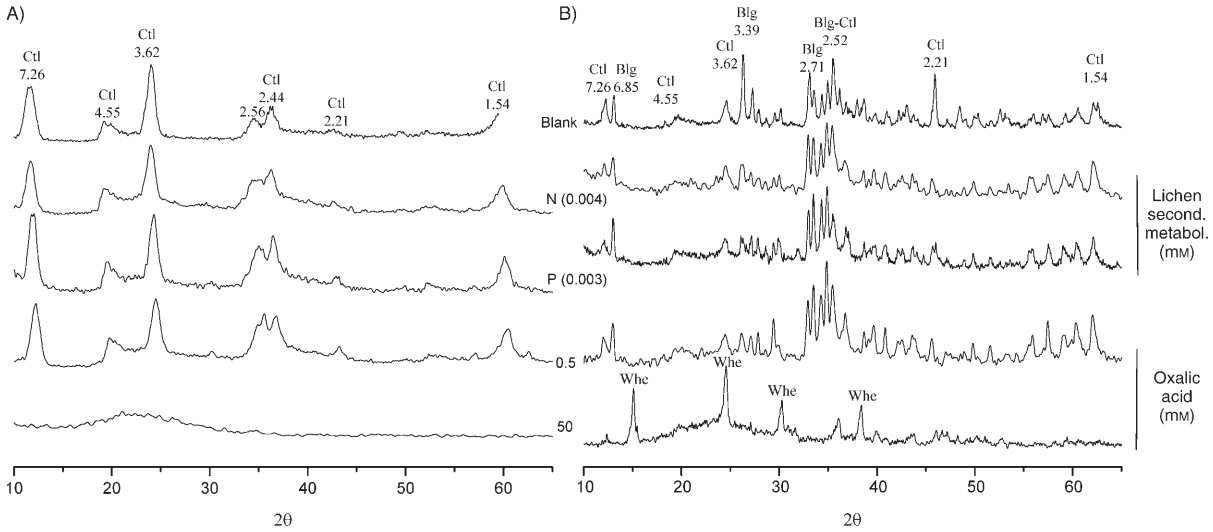

Figure 4. XRD pattern of solid residuals of A) pure chrysotile and B) chrysotile–balangeroite after incubation with deionised water (blank), norstictic acid (N, approximately 0.004 mM), pulvinic acid (P, approximately 0.003 mM) or oxalic acid (0.5 and 50 mM) solutions for 35 d in the dark. Only the main peaks of chrysotile (Ctl) and balangeroite (Blg) are marked and d_{hkl} values reported. Whe: whewellite, $CaC_2O_4{\cdot}H_2O$ (calcd $d_{hkl}=5.29, 3.62, 2.97, 2.35$).

opside (CaMg–pyroxene) and/or calcite ($CaCO_3$) as impurities in the examined sample and to the lower solubility of $CaC_2O_4{\cdot}H_2O$ (whewellite, $K_{sp}=2.3\times10^{-9}$) with respect to $MgC_2O_4{\cdot}2H_2O$ (glushinskite, $K_{sp}=8.6\times10^{-5}$).[39]

Other neo-formed but less abundant compounds were detected by micro-Raman spectroscopy. Hematite (Fe_2O_3, Figure 5, spectrum a) was found in the residuals of both

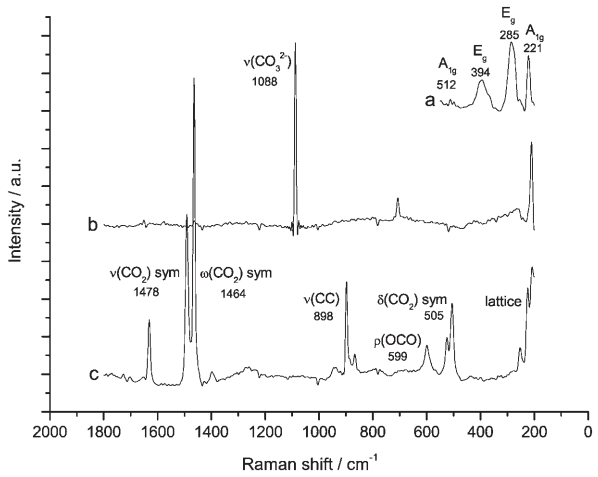

Figure 5. Micro-Raman spectra of neo-formed phases after treatment of chrysotile–balangeroite with oxalic acid: a) hematite; b) carbonate, probably dolomite; c) glushinskite.

samples, subsequent to the incubation with all lichen metabolites. Dolomite ($CaMg(CO_3)_2$, Figure 5, spectrum b) and glushinskite ($MgC_2O_4{\cdot}2H_2O$, Figure 5, spectrum c) were detected in both samples after leaching with 0.5 and 0.05 mM oxalic acid.

Modification induced in surface properties

Coordination state of iron from NO absorption: The topmost layers in minerals are structurally and/or chemically different from the bulk, with ions exhibiting partial coordinative unsaturations.[40] The degree of structural ligand loss is due to the mineral microtopography and varies according to the location of the ions at the surface (for example, on extended surfaces, edge or corner positions). According to their coordination state, metal ions at the surface will show differences in their redox potential. In moist air or in an aqueous medium, the structural coordinative vacancies of these ions are partially replaced by molecular water or hydroxy groups.[40]

Such surface ions are involved in redox or charge-transfer reactions, which may occur at the fibre–living-matter interface, and are responsible for the chemical reactivity towards a variety of endogenous molecules, such as H_2O_2, NO, proteins, lipids and nucleic acids.[7,9,13] Through ligand displacement, endogenous target molecules and functional groups may replace the water molecules and hydroxy groups that saturate the relevant coordinative positions.

It is rather difficult to evaluate at the molecular level the coordinative unsaturations of the iron ions on a hydrated surface directly from the fibres. Therefore, we have here adopted an indirect method, previously described for asbestos and other fibrous minerals[41–43] and typically applied for studying the surface centres of heterogeneous catalysts.[44] The nature and abundance of the surface active sites have been evaluated by means of the adsorption of nitric oxide as a probe molecule, commonly employed on iron centres of various materials.[45–47] The fibre surface was previously deprived of the adsorbed molecules by outgassing under vacuum. The coordinative unsaturations created in such a way were filled by NO molecules, the vibrational features of

which depend on the characteristics of the related surface centre. The amount of gas adsorbed allows evaluation of the abundance of surface active ions.[48] Surface iron ions detected by NO under these conditions are all in the +2 oxidation state, because of the reduction of surface Fe^{3+}, if any, to Fe^{2+} during outgassing at high temperature, as observed for other transition-metal ions. Such alteration of the redox nature of a part of the surface iron ions, however, does not affect the monitoring of their coordination to the surface.[42]

IR spectra of adsorbed NO: *Pure chrysotile (A)*: The IR spectrum of molecular species adsorbed on pure chrysotile in the presence of 30 Torr of NO is shown in Figure 6. NO adsorption on iron sites results in a very weak and broad band at about 1809 cm^{-1} (solid line)[48] which partially decreases after outgassing at room temperature (dotted line). The formation of nitrosylic adducts [Fe–$(NO)_x$] is accompanied by the formation of several other species which produce a complex spectral pattern between 1400–1100 cm^{-1}. Such bands indicate the occurrence of NO_2^- and/or NO_3^- following the oxidation of NO on a few MgO basic sites.[48–50] A partial decomposition of the brucitic layer during outgassing at 400 °C accounts for the presence of MgO in the system. Although chrysotile is generally reported to persist at temperatures higher than 400 °C,[51,52] the same behaviour was observed by some of us with a pure, synthetic chrysotile with a low iron content.[53]

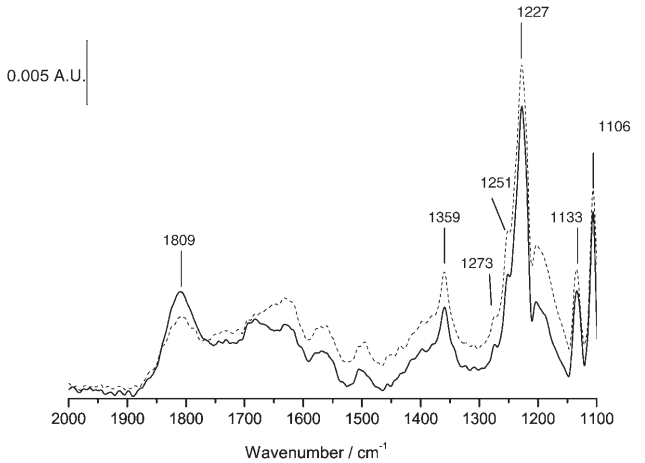

Figure 6. FTIR spectra of surface adsorbed species on pure chrysotile fibres (outgassed at 400 °C for 30 min, supported on an IR transparent silicon plate), in the presence of 30 Torr of NO (—— the gas spectral pattern was subtracted) and after 20 min in vacuum (-----). Only the weak and broad band at 1809 cm^{-1} is due to the formation of nitrosylic complexes at the chrysotile surface.

Since the surface structure was modified following the activation step, the leached samples were not analysed. Some data on the state of the iron ions were nevertheless obtained by means of diffuse-reflectance UV/Vis spectroscopy (data and methods in the Supporting Information). Reflectance spectra, reported as Kubelka–Munk functions, show a decrease in the iron content only after incubation with 50 mM oxalic acid. The spectral features between 30000–20000 cm^{-1} confirm the occurrence of iron oxyhydroxides on the surface of the fibres incubated with 0.5 mM oxalic acid, as detected by micro-Raman spectroscopy.

Chrysotile–balangeroite (B): The IR spectra of adsorbed NO, recorded at decreasing NO coverage values, on chrysotile–balangeroite fibres are shown in Figure 7. In the presence of 30 Torr of NO, the IR spectrum exhibits a main peak at 1803 cm^{-1}, with a shoulder at approximately 1815 cm^{-1}, accompanied by a band at 1732 cm^{-1} and a weak and broad component at approximately 1900 cm^{-1} (Figure 7, spectrum a). A weak component, due to some coadsorbed molecular water, is present at approximately 1630 cm^{-1}. With the NO pressure diminished from 30 down to 0.5 Torr, the intensity of the component at 1800 cm^{-1} decreases and the broad band at approximately 1900 cm^{-1} disappears, while the band at 1735 cm^{-1} conversely increases in intensity (Figure 7, spectra a–j). From 0.5 Torr down to vacuum conditions, the decrease in intensity of the main band at 1812 cm^{-1} (Figure 7, spectra j–n) is not associated to any other spectral change.

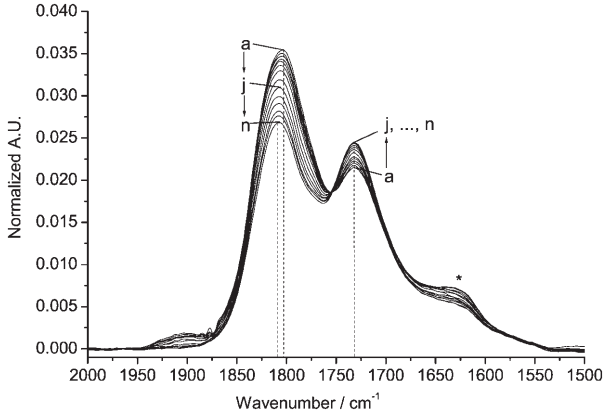

Figure 7. FTIR spectra of NO adsorbed on chrysotile–balangeroite fibres outgassed at 400 °C for 30 min. IR spectra recorded under decreasing coverage of NO, from curve a at 30 Torr to curve j at 0.5 Torr and from curve j at 0.5 Torr to curve n under vacuum. The weak and broad component labelled with * is due to some water molecules coadsorbed on the fibre surface. Spectra intensity were normalised with respect to the mass of the sample.

On the basis of previous studies, including those with other types of asbestos,[41,42] the observed spectral pattern, which is very similar to that reported for pure balangeroite,[43] can be interpreted as resulting from the superposition of three components (Figure 8A): trinitrosyls [Fe^{2+}_A–$(NO)_3$] (with bands at 1803 and 1900 cm^{-1} (weak)), dinitrosyls [Fe^{2+}_B–$(NO)_2$] (with a band at 1732 cm^{-1}, plus a hidden weaker partner in the 1830–1820 cm^{-1} region) and mononitrosyls [Fe^{2+}_C–NO] (with a shoulder at approximately 1810 cm^{-1}).

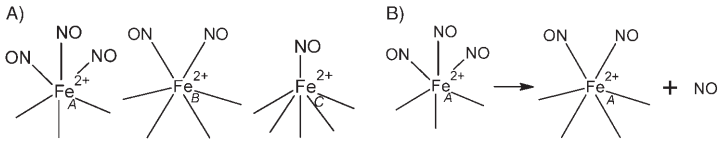

Figure 8. A) Tri-, di-, and mononitrosylic adducts on surface partially uncoordinated iron ions. B) The conversion of the trinitrosylic adduct on Fe^{2+}_{A} sites into dinitrosyls.

The simultaneous presence of the three independent types of nitrosylic adducts documents three types of iron centres that differ in their coordination to the surface.[46,47,54] The lower the coordination, the higher the number of coordinative positions occupied by adsorbed NO. Surface Fe^{2+} sites yielding tri-, di- and mononitrosyls will hereafter be referred to as Fe^{2+}_{A}, Fe^{2+}_{B} and Fe^{2+}_{C}, respectively (Figure 8A).[41]

By decreasing the NO pressure from 30 to 0.5 Torr, the occurrence of a spectral component, superimposed on to the band of Fe^{2+}_{B} dinitrosyls, accounts for a conversion of trinitrosyls on Fe^{2}_{A} sites into dinitrosyls (Figure 8B).

Further changes at lower NO coverage (from 0.5 Torr to vacuum), only involving the main spectral component at approximately 1815 cm^{-1}, indicate the presence on the surface of a fraction of Fe^{2+}_{C} mononitrosyls with more reversible adsorption than that of the Fe^{2+}_{A} and Fe^{2+}_{B} dinitrosyls. This peculiar feature was previously observed on balangeroite[43] but has not been observed on other asbestos fibres, including UICC chrysotile (UICC = Union Internationale Contre le Cancer). NO adsorption on the chrysotile–balangeroite most likely occurs on balangeroite.

The infrared spectra of NO adsorbed on the samples leached with norstictic acid, pulvinic acid and 0.5 and 50 mM oxalic acid solutions (Figure 9A–D, respectively) highlight the modifications induced by lichen metabolites on the coordination state of the iron ions exposed at the surface.

Under an NO coverage of 30 Torr, the recorded spectra (Figure 9A–C, spectrum a) are similar to that observed for the non-leached sample (Figure 7, spectrum a). Conversely, the subsequent decrease of NO pressure does not result in any increase in the dinitrosyl signal, a result indicating that trinitrosylic adducts, expected to form under high NO coverage and to convert into dinitrosyls by lowering the NO pressure, are not present at the surface of the leached samples. On this basis, the main band at approximately 1804 cm^{-1} should mainly contain a vibrational contribution from the mononitrosylic adducts formed on Fe^{2+}_{C} sites.

The adsorption of NO (30 Torr) on the sample incubated with 50 mM oxalic acid (Figure 9D) induces a small but still detectable formation of very stable mononitrosylic adducts on type C iron sites. This indicates that iron is drastically removed by the leaching process with 50 mM oxalic acid solution but some traces still remain.

Free-radical release (Fenton activity): Several asbestos minerals are highly reactive in releasing free radicals by reacting with several target molecules.[43,55,56] Among the usually investigated radical-generating mechanisms, we examined the

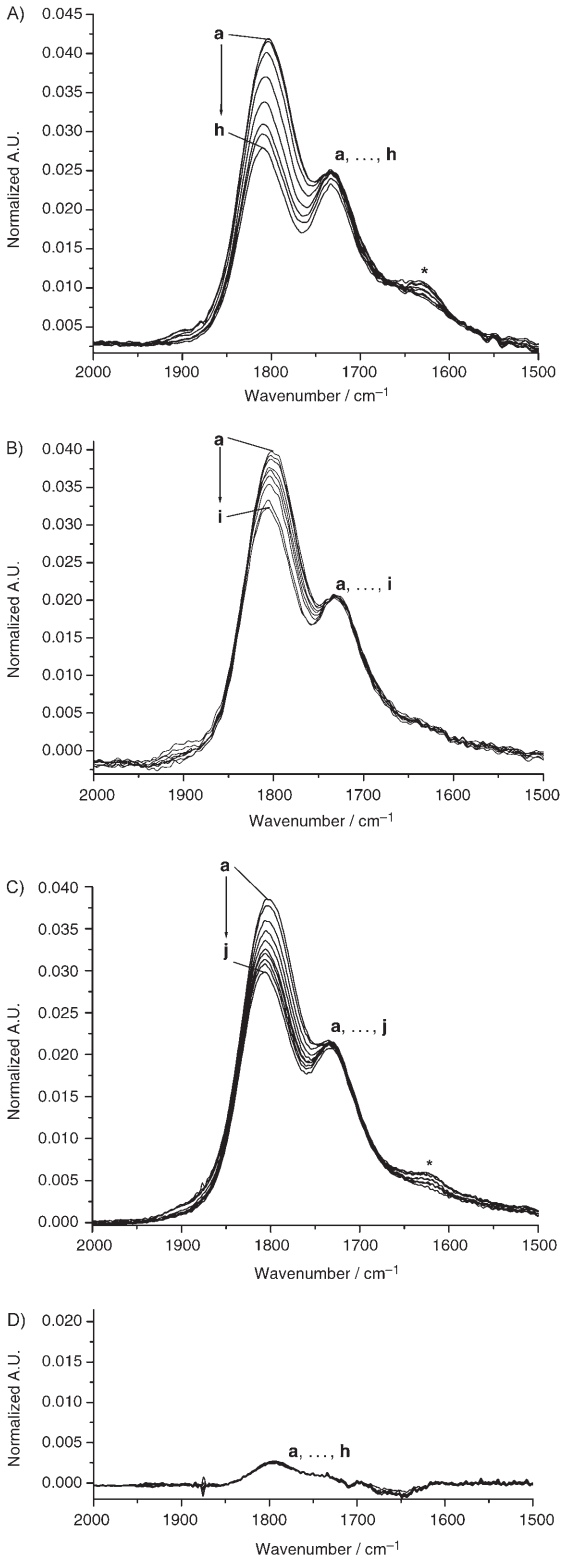

Figure 9. FTIR spectra of NO adsorbed on chrysotile–balangeroite fibres incubated with A) norstictic acid, B) pulvinic acid, C) 0.5 mM and D) 50 mM oxalic acid solutions. Self-supporting pellets of leached fibres were outgassed at 400 °C for 30 min. IR spectra were recorded in the presence of decreasing pressures of NO, from curve a at 30 Torr to vacuum conditions (curves h, i, j and h in A–D, respectively). * indicates some coadsorbed water molecules. Spectra intensities were normalised with respect to the mass of the sample.

release of ·OH radicals in the presence of hydrogen peroxide (the Fenton activity).[56,57] This test mimics the contact with lysosomal fluids, following phagocytosis by alveolar macrophages, where H_2O_2 is released. The results are shown in Figure 10A and B for pure chrysotile and chrysotile–balangeroite, respectively.

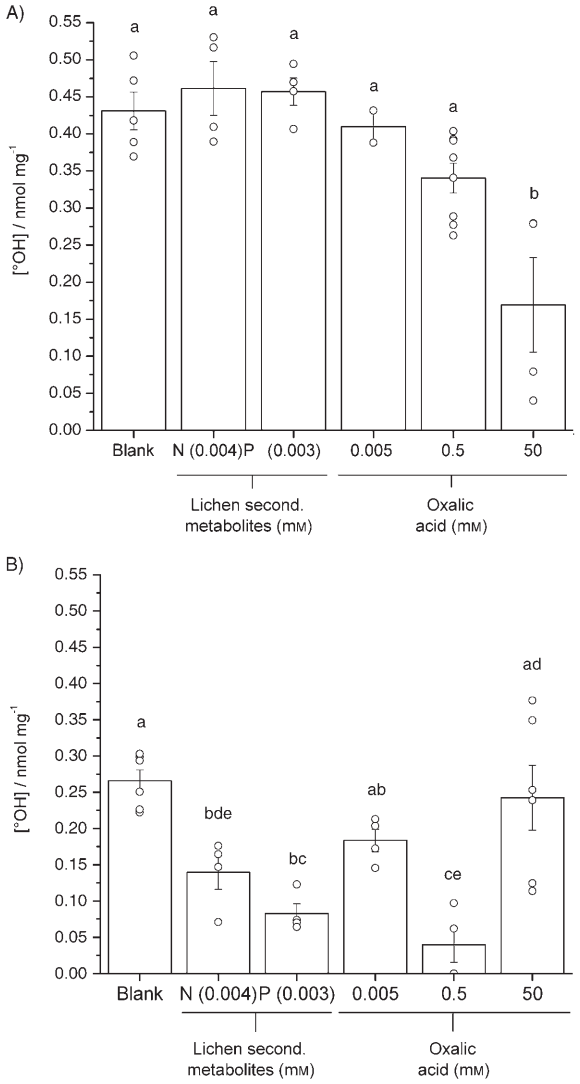

Figure 10. ·OH concentration measured by EPR spectroscopy by suspending A) pure chrysotile and B) chrysotile–balangeroite in a hydrogen peroxide solution, after 30 min of reaction. Each sample was incubated with water (blank), lichen secondary metabolites (N: norstictic acid; P: pulvinic acid) or primary metabolite (oxalic acid). The empty bars indicate, as nmol normalised per mg of fibres, the amount of ·OH radicals generated. Data are reported as means ± the standard error of at least three independent measures, performed for each treated sample. The result of each single measurement was also reported in order to highlight the strong variability occurring in natural samples (○). According to Tukey's test (ANOVA), bars which do not share at least one letter are statistically different.

Pure chrysotile (A): Untreated samples (Figure 10A, blank) exhibit an intense generation of ·OH, due to the Fenton-like reactivity of iron ions exposed at the fibre surface. The ·OH radical release is significantly decreased after leaching with 50 mM oxalic acid, even though a wide range of variability is observed. The EPR spectra obtained for pure chrysotile leached with norstictic acid, pulvinic acid and 0.005 and 0.5 mM oxalic acid are not significantly different from the fibres incubated in pure water (blank), although a slight decreasing trend of the mean values is observed with increasing concentrations of oxalic acid.

Chrysotile–balangeroite (B): The fibres incubated in deionised water (Figure 10B, blank) are active in the Fenton-like generation of ·OH radicals, although the released amount is significantly lower than that with the pure chrysotile. The use of 0.005 mM of oxalic acid does not affect the Fenton activity of the fibres. The samples leached with secondary metabolites (norstictic acid and pulvinic acid) and with 0.5 mM oxalic acid exhibit a significant reduction in reactivity, with respect to the blank. The leaching with 50 mM oxalic acid solution restores the Fenton activity of chrysotile–balangeroite, probably because of the presence of a few poorly coordinated iron ions still present at the surface of the neoformed silica phase.

Discussion

Chemical substitution of magnesium in the chrysotile structure is limited by its peculiar crystallographic feature.[58] Chrysotile mostly contains iron up to 2 wt%, as in the case of the pure sample from Val Malenco, Italy ($FeO_{tot} \approx 1.8$ wt%), but some specimens may contain up to 6 wt%.[51] Chrysotile ($FeO_{tot} \approx 5.6$ wt%) from the Balangero asbestos mine belongs to this latter group of fibrous serpentine asbestos and is associated with the iron-rich asbestiform mineral balangeroite.

Although asbestos reactivity is commonly related to its iron content,[7,13] the quantity of ·OH radical released by the two samples appears to be inversely related to their FeO_{tot} wt% value. This result, in agreement with previous findings by some of us, correlates with a recent study on synthetic iron-doped chrysotile which gives evidence for increasing reactivity with a decrease in the iron content from 1.25 wt% down to 0.25 wt%.[53] With regard to the chrysotile–balangeroite sample, it is worth noting that both chrysotile and balangeroite are known to react with H_2O_2 releasing ·OH,[43,57] thus suggesting that both phases are involved in the chemical reactivity. The characterisation of the iron coordinative state for this mixed sample indicates the presence on the surface of three types of iron centres with one, two or three coordinative unsaturations toward the surface.[41] The occurrence of highly uncoordinated iron ions (Fe^{2+}_A) accounts for the detected Fenton activity.

The leaching action of lichen metabolites on the surface and within the bulk of the fibre induces different modifications in the two fibre types in both chemical composition and Fenton activity. The results on the leaching of chrysotile

and of chrysotile–balangeroite are therefore discussed separately.

Leaching effects on pure chrysotile: A reduction in the Fenton activity of the fibres is obtained after leaching only with 50 mM oxalic acid, when the brucite-like layer is solubilised and the crystalline structure is lost. Complete depletion of magnesium and iron is indicated by the zeroing of their atomic ratios with respect to silicon. Iron depletion is also confirmed by the spectral modification observed with reflectance spectroscopy.

A significant leaching of the brucitic layer is also detected after incubation with 0.5 mM oxalic acid, as indicated by the high magnesium content found in the supernatant. The decrease of the Mg/Si and Fe/Si ratio indicates that the dissolution of the brucite-like layer proceeds incongruently with the consequent formation of surface phases impoverished in divalent cations. Nevertheless, fibre crystallinity is unchanged on the whole. Under these conditions, the Fenton activity of the fibres is not affected.

The leaching action of oxalic acid toward chrysotile was reported in some pioneering studies.[34,59–61] Morgan et al.[62] and Monchaux et al.[63] had shown that a loss of carcinogenic potency is achieved in chrysotile after an extensive transformation of the bulk (Mg depletion $>80\,\%$). Our observations suggest that only by zeroing the iron content, which follows the magnesium depletion, is a significant reduction in Fenton activity achieved, a fact confirming that iron is the key ion to be removed in a detoxification process. It is worth noting that fibres leached with 0.5 mM oxalic acid are very differently modified. According to Johan et al.[59] and Hochella,[64] chelating molecules do not act homogeneously from fibre to fibre. Indeed, when leaching of magnesium from chrysotile fibres was studied by Jaurand et al.,[65,66] it was found that the amount of leaching varied for each fibre and also along the length of a single fibre. Such variability is likely to cause the wide error bars reported in these experiments.

The leaching processes accomplished with lichen secondary metabolites and 0.005 mM oxalic acid do not alter the Fenton activity of the fibres. A selective dissolution of the brucitic layer is responsible for the enrichment in magnesium of the supernatant, although the constant atomic ratios in the bulk analyses indicate that this process only involves a few surface layers.

Leaching effects on chrysotile–balangeroite: A reduction in Fenton activity is observed on fibres leached with 0.5 mM oxalic acid and with lichen secondary metabolites. In all leached fibres, the coordinative state of iron at the surface is modified, as detected by the adsorption of an iron-specific molecular probe (NO). Trinitrosylic adducts are no longer observed upon adsorption of NO on such modified samples. This finding accounts for the loss of the highly uncoordinated iron ions (assigned as Fe^{2+}_{A}), due to the chelating effects of oxalic acid and lichen secondary metabolites. Ions with a higher coordinative unsaturation are more easily extracted by chelating agents.[41] The lower the coordination at the surface, the higher the redox reactivity of ions,[41] so the removal and/or masking of the less coordinated iron ions is an important step in fibre detoxification. A similar chelating and masking synergic action was previously reported for desferrioxamine and ferrozine on crocidolite asbestos.[12,67]

In some pioneering studies, leached chrysotile exhibited a reduced cytotoxicity[63] and a decreased potential to induce mesothelioma in rats.[68] Such effects were ascribed to the chelator-driven rupture of the crystalline framework and its whole conversion into the debris of amorphous silica. By examining the effects of lichen metabolites on chrysotile and by studying the surface properties of leached minerals, we have herein highlighted the fact that a chemical inactivation process follows the modification in the state of iron at the surface of the chrysotile fibres and/or of the associated iron-rich minerals (that is, balangeroite).

The acidic and chelating properties of oxalic acid[60] induce, through an erosion of the sub-surface layers, a depletion in magnesium in the brucite-like layer of chrysotile. The Mg depletion similarly affects the two minerals leached with secondary metabolites and 0.005 mM oxalic acid. This can be related to a first leaching step of the outer brucitic layers. A wider stability threshold follows this first step, as reported for other Mg and Mg–Fe silicates.[37] By incubating pure chrysotile in 0.5 mM oxalic acid, this stability threshold is exceeded. By contrast, chrysotile–balangeroite is more inert toward oxalic acid than pure chrysotile, since a vast depletion in Mg is observed only after leaching with the 50 mM solution. The composition of the chrysotile phase in the chrysotile–balangeroite sample after the inactivation treatment with 0.5 mM oxalic acid, however, approximates the composition of fibres which were described below lichen thalli from the Balangero asbestos mine.[29]

A congruent dissolution takes place on the chrysotile–balangeroite sample: release of silicon in parallel with the leaching of the brucitic layer occurs even after incubation with low concentrations of lichen substances (that is, secondary metabolites and diluted oxalic acid solutions). In contrast to the pure chrysotile results, in which the brucitic layer is selectively removed, the intimate association of chrysotile to balangeroite is likely to induce a different surface exposure of Mg and Si to the chelating agents, which would account for such a different behaviour.

It is worth noting that modifications induced by lichen secondary metabolites, although limited to the uppermost surface layer, are sufficient to reduce the Fenton activity. The chelating properties of lichen secondary metabolites[26,69] are related to the presence of OH and COOH functional groups.[27] Cu–norstictic acid complexes were detected in lichens colonising Cu-rich rocks.[70] The very low solubility of these molecules in water, however, has led to a wide disregard for their weathering properties.[22,71] The unmodified chemical composition of the bulk also indicates weak extraction potential; however, to the best of our knowledge, this is the first evidence of the role of lichen secondary metabolites in surface chemistry. Since they were

recognised within weathered rocks,[28] they could act as proton sources or as ligands, thus finally contributing to the chemical weathering processes.

The incubation with lichen metabolites, and in particular with pulvinic acid, is associated with some significant increases in the iron detected in the SEM-EDS analyses of the fibres. Probably due to a templating action of adsorbed organic molecules on the fibres,[72] iron solubilised by lichen metabolites mainly reprecipitates as hematite on the fibre surface. As well-crystallised iron oxides and hydroxides, which are also abundant at the lichen–rock interface in the field conditions,[22,29] are unreactive and biologically inert,[13,57] this enrichment in iron, as expected, does not affect free-radical release.

Surprisingly, chrysotile–balangeroite leached with 50 mM oxalic acid shows a variable but significant restoration of the Fenton activity. Such variability often occurs in the presence of iron removal/deposition equilibria because only small fractions of isolated iron ions are catalytic centres for radical generation.[56] Accordingly, low concentrations of highly dispersed iron ions in a silica matrix were previously reported as strongly active in free-radical release.[73] During iron removal the number of such sites is bound to vary, occasionally increasing and then declining, on a given patch of fibre surface. Iron depletion in both the chrysotile and balangeroite phases has been directly detected at the bulk level, but the low formation of Fe nitrosyls accounts for the persistence of iron traces on the surface of the sample. The chrysotile–balangeroite mineral relics, however, after the incubation with 50 mM oxalic acid have lost both their crystalline structure and fibrous habit, which are main factors in asbestos pathogenicity. To represent field conditions, 50 mM oxalic acid could be considered as representative of a very long-term bioweathering exposure.

Conclusion

By mimicking the weathering effect of lichens on chrysotile, the present study highlights a surface inactivation process of chrysotile due to modification of the coordinative state of iron, consequent to a substantial removal of magnesium ions. The process takes place at the surface of chrysotile itself and/or of its associated iron-rich minerals (that is, balangeroite). The induced alterations are observed after incubation with lichen metabolite solutions at very low concentrations, when the rupture of the chrysotile silica framework and the full inactivation of the fibres is far from being achieved. Under these circumstances, the least coordinated iron ions, that is, the most reactive ones, appear to be removed. Consequently, Fenton-like activity, a process widely correlated with asbestos pathogenicity, is progressively reduced.

Primary and secondary lichen metabolites, the latter often disregarded as weathering agents, affect the surface reactivity of chrysotile fibres. The effect is more pronounced on chrysotile–balangeroite than on pure chrysotile, a result indicating that the specific chemical features of each chrysotile source should be independently considered with regard to inactivation.

The present study—the first attempt, to our knowledge, to reproduce in the laboratory the chemical modifications induced by lichens on asbestos—confirms lichens as possible bioattenuating microorganisms for asbestos-polluted rocks; the lichens modify fibre reactivity and ultimately transform fibres into amorphous non-toxic silica debris.

Experimental Section

Asbestos samples: Samples from two different asbestos-rich outcrops were employed (Table 1):

Table 1. Representative quantitative analyses of the asbestos minerals investigated (wt%; SEM-EDS analyses).

	Pure chrysotile Ctl $[Mg_3Si_2O_5(OH)_4]$ Oxides wt%	Chrysotile–balangeroite Ctl $[Mg_3Si_2O_5(OH)_4]$ Oxides wt%	 Blg $[(Mg,Fe,Mn,Al)_{42}O_6(Si_4O_{12})_4(OH)_{40}]$ Oxides wt%
SiO_2	43.64	41.49	29.03
Al_2O_3	0.02	2.45	0.08
$FeO_{(tot)}$	1.67	5.76	23.00
MnO	0.00	0.00	2.79
MgO	41.82	37.61	35.15
H_2O	12.80	12.55	9.90
total	99.95	99.96	99.95
Mineral formula	$(Mg_{2.88}Fe_{0.07})Si_{2.02}O_5(OH)_4$	$(Mg_{2.65}Fe_{0.23}Al_{0.13})Si_{1.96}O_5(OH)_4$	$(Mg_{29.32}Fe_{10.77}Mn_{1.32}Al_{0.05})Si_{16.26}O_{54}(OH)_{40}$

1) A relatively pure chrysotile specimen, with limited iron contamination, from the Central Internal Alps (Val Malenco, Sondrio, Italy). N_2-BET specific surface area is 64 $m^2 g^{-1}$.
2) A sample from the Western Internal Alps (asbestos mine of Balangero, Val di Lanzo, Torino, Italy). In this sample, long-fibre chrysotile is intergrown with brown, Fe-rich asbestiform balangeroite.[74] According to XRD diffraction pattern analysis and light-microscopy observation, the chrysotile–balangeroite ratio within the sample is about 3:2. N_2-BET specific surface area is 69 $m^2 g^{-1}$.

Lichen metabolites: Oxalic acid, chosen for its role in lichen and fungi weathering action,[23] was from Merck Pro-analysis. Norstictic acid, known for its chelating properties and naturally recovered Cu complexes, is produced by several lichen species which colonise natural asbestos-rich substrata.[27,70] Norstictic acid was extracted with acetone, following the method of Huneck and Yoshimura,[25] from the lichen *Pleurosticta acetabulum*. This species does not colonise asbestos-rich substrata, but it contains only norstictic acid as a secondary metabolite;[75] therefore, no purification procedures were required. Pulvinic acid was extracted from the lichen *Candelariella vitellina*, which commonly colonises asbestos-rich substrata and is active in weathering chrysotile fibres[29] but does not se-

crete oxalic acid. After the extraction, the norstictic and pulvinic acid crystals were dissolved in water, the solutions were filtered, the purity was checked by means of TLC,[76] and the concentrations were measured spectrophotometrically at 256 and 239 nm, respectively.[25]

Reagents: 5,5-Dimethyl-1-pyrroline-1-oxide (DMPO) was from Alexis-biochemicals (CA, USA). To minimise contamination by degradation products, DMPO was purified by a pass through charcoal, according to the method proposed by Buettner and Oberley,[77] and stored in the dark at 4 °C. All other reagents were purchased from Sigma–Aldrich. For all experiments, ultrapure MilliQ water was used.

Separation and incubation of asbestos fibres: Small bundles of pure chrysotile and chrysotile–balangeroite were firstly separated from serpentinite rocks with Teflon pincers and gently crushed in order to further isolate the fibres and favour a good dispersion during the leaching experiments. The fibres were then suspended in solutions of oxalic acid at different concentrations (0.005, 0.5 and 50 mM), of norstictic acid at approximately 0.004 mM and of pulvinic acid at approximately 0.003 mM. The solid/liquid ratio was 1 mg mL^{-1}. To simulate the concentration gradient occurring in field conditions, the experiments were performed in a static medium (at 25 °C, in the dark). The initial pH values were 5.9, 4.5 and 1.6 for 0.005, 0.5 and 50 mM oxalic acid solutions, respectively; the initial pH value for both secondary metabolite solutions was about 6.5. Sodium formaldehyde (1 %) was always added to the incubating solutions as an antiseptic agent. After 35 days of incubation, the fibres were filtered and dried, without rinsing, in order not to dissolve the neo-formation mineral phases possibly precipitated during the experiment.

Analytical techniques

ICP-AES and SEM-EDS: Inductively coupled plasma atomic emission spectrometry (ICP-AES) analyses and energy dispersive X-ray spectroscopy (EDS) coupled with scanning electron microscopy (SEM) were performed on the organic-acid solution filtrates and on the fibre solid residuals of the fibres, respectively, in order to evaluate the leaching effects of the lichen metabolites.

ICP-AES analyses of magnesium and silicon were performed with a Liberty 100 Varian apparatus equipped with a V-Groove nebuliser and a Czerny–Turner monocromator. The coolant flow was 15 L min^{-1}. The analytical wavelengths adopted were $\lambda = 251.611$ nm for silicon and $\lambda = 285.213$ nm for magnesium. All determinations were carried out with a nebuliser pressure of 120 kPa, at a viewing height of 8 mm, with an integration time of 1 s and an induction power of 1 kW.

SEM-EDS observation and elemental analysis were performed on carbon-coated samples with a Stereoscan S360 Cambridge electron microscope equipped with an Energy 200 Oxford Instruments EDS apparatus. The accelerating voltage was 15 kV and the secondary electron detector was used. During EDS analyses, the counting time was 50 s; pure oxides were used as standards. Data were collected by using a Microanalysis Suite Issue 12 (INCA Suite, version 4.01, Oxford Instruments) system.

XRD and micro-Raman spectroscopy: X-ray diffraction (XRD) and micro-Raman spectroscopy were used as complementary techniques in order to evaluate the occurrence of neo-formed phases after the suspension of the fibres in the organic-acid solutions. XRD analyses were performed on the solid residuals with a Siemens D5000 apparatus, with $\theta-2\theta$ geometry and Cu Kα radiation. The patterns obtained were recognised by comparison with those contained in the Joint Committee of Powder Diffraction Standard (JCPDS) archives.

Raman spectra of precipitates on the leached samples were collected with a LabRam HR800 micro-Raman spectrometer (Jobin Yvon) equipped with an HeNe laser at an excitation wavelength of 632.8 nm, a CCD detector and an Olympus BX41 optical microscope. The spectra were compared with those contained in references [78] and [79] and in the Raman Spectra Database of Minerals and Inorganics.[80]

Electron paramagnetic resonance spectroscopy (EPR) and spin trapping: In order to detect the formation of the $^{\bullet}$OH radical in aqueous suspensions of the fibres in the presence of H_2O_2 (the Fenton activity), the spin-trapping agent DMPO, which gives a relatively stable [DMPO−OH]$^{\bullet}$ adduct, was used. Following a well-established technique described in previous studies,[55] the nature and quantity of the stabilised radical was measured by means of EPR spectroscopy.

Fibres were suspended (22 mg mL^{-1}) in H_2O_2 (0.250 mL, 0.5 M in H_2O), DMPO (0.250 mL, 0.05 M) and phosphate buffer (0.500 mL, 1 M, pH 7.4). The radical formation was evaluated by recording the EPR spectrum of the [DMPO-OH]$^{\bullet}$ adduct at 10, 30 and 60 min. All spectra were recorded on a Miniscope MS 100 (Magnettech, Berlin, Germany) EPR spectrometer. The instrument settings were as follows: microwave power, 10 mW; modulation, 1000 mG; scan range, 120 G; centre of field, approximately 3345 G. The number of radicals released is proportional to the intensity of the EPR signal. The signals were double integrated and numeric values were reported, as arbitrary units, in order to quantitatively represent the production of free radicals by the mineral fibres. Blanks were performed in parallel in the absence of any fibre. All the experiments were repeated at least twice.

IR spectroscopy

Adsorption of NO as a molecular probe for surface iron (IR-NO): The IR spectra (4 cm^{-1} resolution) of the fibres, in the form of self-supporting pellets, were obtained by means of a Bruker IFS28 spectrometer (FT-IR) equipped with an MCT detector. Previous studies on crocidolite asbestos[42] and UICC chrysotile (unpublished data) suggested outgassing in vacuo at 400 °C as the most favourable activation step before NO adsorption, because this allows the highest degree of removal of water molecules and hydroxy groups adsorbed onto iron ions. The fibres placed in the IR cell were connected to a conventional vacuum line (residual pressure: 1.0×10^{-6} Torr; 1 Torr = 133.33 Pa) and were outgassed at 400 °C for 45 min.

IR spectra were recorded in the presence of decreasing equilibrium pressures of NO (from 30 Torr to vacuum) at room temperature. The spectra of adsorbed NO are reported in absorbance units, after subtraction of the spectrum of the fibres before NO adsorption and of NO gas itself.

Acknowledgements

This research has been carried out with the financial support of Regione Piemonte, "Direzione regionale 22, Tutela e Risanamento Ambientale–Programmazione–Gestione Rifiuti", in the context of a multidisciplinary project "Asbestos hazard in Western Alps". F.T. and S.E.F.-L. are the recipients of a postdoctoral fellowship from Regione Piemonte within the framework of the project. This work was also partially supported by PRIN project no. 20022055875-003. The authors are grateful to Professor C. Rinaudo for Raman spectroscopy, to Dr. M. Bergamini (RSA Balangero) for admission to the mine and to Professor R. Compagnoni for helpful discussions.

[1] I. J. Selikoff, J. Churg, E. C. Hammond, *JAMA, J. Am. Med Assoc.* **1964**, *188*, 22–26.
[2] *Monographs on the Evaluation of the Ccarcinogenic Risk of Chemicals to Man: Asbestos*, Centre International de Recherche sur le Cancer–IARC, Lyon (France) **1977**, pp. 1–106.
[3] L. Kazan-Allen, *Lung Cancer* **2005**, *49 (Suppl. 1)*, S3–8.
[4] A. B. Kane, *Mechanisms of Mineral Fibre Carcinogenesis, Vol. 140* (Eds. A. B. Kane, P. Boffetta, R. Saracci, J. D. Wilbourn) Centre International de Recherche sur le Cancer–IARC, Lyon (France), **1996**, p. 11.
[5] B. T. Mossman, A. Hubbard, A. Shukla, C. R. Timblin, *Inhalation Toxicol.* **2000**, *12*, 307–316.
[6] W. J. Nicholson, *Ind. Health* **2001**, *39*, 57–64.
[7] J. A. Hardy, A. E. Aust, *Carcinogenesis* **1995**, *16*, 319–325.
[8] B. T. Mossman, A. Churg, *Am. J. Respir. Crit. Care Med.* **1998**, *157*, 1666–1680.
[9] B. Fubini, C. Otero-Areán, *Chem. Soc. Rev.* **1999**, *28*, 373–381.
[10] P. J. Landrigan, M. Soffritti, *Am. J. Ind. Med.* **2005**, *47*, 471–474.
[11] L. G. Lund, A. E. Aust, *Carcinogenesis* **1992**, *13*, 637–642.

[12] B. Fubini, *Environ. Health Perspect.* **1997**, *105 (Suppl. 5)*, 1013–1020.
[13] D. W. Kamp, S. A. Weitzman, *Thorax* **1999**, *54*, 638–652.
[14] V. A. Kostyuk, A. I. Potapovich, E. N. Vladykovskaya, M. Hiramatsu, *Planta Med.* **2000**, *66*, 762–764.
[15] I. Poser, Q. Rahman, M. Lohani, S. Yadav, H. H. Becker, D. G. Weiss, D. Schiffmann, E. Dopp, *Mutat. Res.* **2004**, *559*, 19–27.
[16] S. Daghino, E. Martino, I. Fenoglio, M. Tomatis, S. Perotto, B. Fubini, *Chem. Eur. J.* **2005**, *11*, 5611–5618.
[17] E. Martino, S. Cerminara, L. Prandi, B. Fubini, S. Perotto, *Environ. Toxicol. Chem.* **2004**, *23*, 938–944.
[18] E. Martino, L. Prandi, I. Fenoglio, P. Bonfante, S. Perotto, B. Fubini, *Angew. Chem.* **2003**, *115*, 229–232; *Angew. Chem. Int. Ed.* **2003**, *42*, 219–222.
[19] S. Daghino, F. Turci, M. Tomatis, A. Favier, S. Perotto, T. Douki, B. Fubini, *Environ. Sci. Technol.* **2006**, *40*, 5793–5798.
[20] Lichens and the biodeterioration of stonework: the Italian experience: R. Piervittori in *Biodeterioration of Stone Surfaces* (Eds.: L. L. St. Clair, M. R. D. Seaward), Kluwer Academic Publishers, Dordrecht, **2004**, pp. 45–68.
[21] *Biodeterioration of Stone Surfaces* (Eds.: L. L. St. Clair, M. R. D. Seaward), Kluwer Academic Publishers, Dordrecht, **2004**.
[22] P. Adamo, P. Violante, *Appl. Clay Sci.* **2000**, *16*, 229–256.
[23] E. Hoffland, T. W. Kuyper, H. Wallander, C. Plassard, A. A. Gorbushina, K. Haselwandter, S. Holmstrom, R. Landeweert, U. S. Lundstrom, A. Rosling, R. Sen, M. M. Smits, P. A. van Hees, N. van Breemen, *Front. Ecol. Environ.* **2004**, *2*, 258–264.
[24] K. Mosbach, *Acta Chem. Scand.* **1967**, *21*, 2331–2334.
[25] S. Huneck, Y. Yoshimura, *Identification of lichen substances*, Springer Verlag, Berlin, **1996**.
[26] I. K. Iskandar, J. K. Syers, *J. Soil Sci.* **1972**, *23*, 255–265.
[27] C. Ascaso, J. Galvan, *Pedobiologia* **1976**, *16*, 321–331.
[28] T. Bjelland, I. H. Thorseth, *Chem. Geol.* **2002**, *192*, 81–98.
[29] S. E. Favero-Longo, F. Turci, M. Tomatis, D. Castelli, P. Bonfante, M. F. Hochella, R. Piervittori, B. Fubini, *J. Environ. Monit.* **2005**, *7*, 764–766.
[30] E. J. W. Whittaker, *Acta Crystallogr.* **1956**, *9*, 855–862.
[31] Z. Elias, O. Poirot, O. Schneider, A. M. Marande, M. C. Daniere, F. Terzetti, H. Pezerat, J. Fournier, R. Zalma, *Cancer Detect. Prev.* **1995**, *19*, 405–414.
[32] J. C. McDonald, A. D. McDonald, J. M. Hughes, *Ann. Occup. Hyg.* **1999**, *43*, 439–442.
[33] E. Gazzano, C. Riganti, M. Tomatis, F. Turci, A. Bosia, B. Fubini, D. Ghigo, *J. Toxicol. Environ. Health Part A* **2005**, *68*, 41–49.
[34] M. J. Wilson, D. Jones, W. J. Mc Hardy, *Lichenologist* **1981**, *13*, 167–181.
[35] B. Fubini, A. E. Aust, R. E. Bolton, P. J. A. Borm, J. Bruch, G. Ciapetti, K. Donaldson, Z. Elias, J. Gold, M. C. Jaurand, A. B. Kane, D. Lison, H. Muhle, *Altern. Lab. Animals (ATLA)* **1998**, *26*, 579–617.
[36] D. Bernstein, V. Castranova, K. Donaldson, B. Fubini, J. Hadley, T. Hesterberg, A. Kane, D. Lai, E. E. McConnell, H. Muhle, G. Oberdorster, S. Olin, D. B. Warheit, *Inhalation Toxicol.* **2005**, *17*, 497–537.
[37] J. Schott, R. A. Berner, E. L. Sjoberg, *Geochim. Cosmochim. Ac.* **1981**, *45*, 2126–2135.
[38] H. L. Zhang, P. R. Bloom, *Soil Sci. Soc. Am. J.* **1999**, *63*, 815–822.
[39] K. W. Whitten, R. E. Davis, L. Peck, G. G. Stanly, *General Chemistry*, Brooks Cole, Belmont, CA, **2003**.
[40] Chemical weathering of silicates in nature: A microscopic perspective with theoretical considerations: M. F. Hochella, J. F. Banfield in *Reviews in mineralogy* (Eds.: A. F. White, S. L. Brantley), The Mineralogical Society of America, Washington, DC, USA, **1995**, pp. 353–406.
[41] G. Martra, M. Tomatis, I. Fenoglio, S. Coluccia, B. Fubini, *Chem. Res. Toxicol.* **2003**, *16*, 328–335.
[42] G. Martra, E. Chiardola, S. Coluccia, L. Marchese, M. Tomatis, B. Fubini, *Langmuir* **1999**, *15*, 5742–5752.
[43] F. Turci, M. Tomatis, E. Gazzano, C. Riganti, G. Martra, A. Bosia, D. Ghigo, B. Fubini, *J. Toxicol. Environ. Health Part A* **2005**, *68*, 21–39.
[44] Catalysis: *Handbook of vibrational spectroscopy—Applications in industry, materials and the physical sciences* (Eds.: J. M. Chalmers, P. R. Griffiths), Wiley, Chichester, UK, **2002**, p. 3005.
[45] G. Busca, V. Lorenzelli, *J. Catal.* **1981**, *72*, 303–313.
[46] S. Yuen, Y. Chen, J. A. Dumesic, N. Topsoe, H. Topsoe, *J. Phys. Chem.* **1982**, *86*, 3022–3032.
[47] F. Boccuzzi, E. Guglielminotti, F. Pinna, M. Signoretto, *J. Chem. Soc. Faraday Trans.* **1995**, *91*, 3237–3242.
[48] K. I. Hadjiivanov, *Catal. Rev. Sci. Eng.* **2000**, *42*, 71–144.
[49] L. Cerruti, E. Modone, E. Guglielminotti, E. Borello, *J. Chem. Soc. Faraday Trans. 1* **1974**, *70*, 729–739.
[50] X. Lu, X. Xu, N. Q. Wang, Q. Zhang, *J. Phys. Chem. B* **1999**, *103*, 5657–5664.
[51] F. J. Wicks, A. G. Plant, *Canadian Mineralogist* **1979**, *17*, 785–830.
[52] B. W. Evans, *Int. Geol. Rev.* **2004**, *46*, 479–506.
[53] F. Turci, PhD Thesis, Università di Torino (Torino), **2006**.
[54] G. Berlier, F. Bonino, A. Zecchina, S. Bordiga, C. Lamberti, *ChemPhysChem* **2003**, *4*, 1073–1078.
[55] B. Fubini, L. Mollo, E. Giamello, *Free Radical Res.* **1995**, *23*, 593–614.
[56] I. Fenoglio, L. Prandi, M. Tomatis, B. Fubini, *Redox Rep.* **2001**, *6*, 235–241.
[57] B. Fubini, L. Mollo, *Toxicol. Lett.* **1995**, *82–83*, 951–960.
[58] Serpentine minerals: structure and petrology: F. J. Wicks, D. S. O'Hanley in *Reviews in Mineralogy* (Ed.: P. H. Ribbe), The Mineralogical Society of America, Washington, DC, USA, **1988**, pp. 113–133.
[59] Z. Johan, J. Goni, C. Sarica, G. Bonnaud, J. Bignon, *Int. Meet. Org. Geochem 6th*, **1973**, 883–903.
[60] J. H. Thomassin, J. Goni, P. Baillif, J. C. Touray, M. C. Jaurand, *Phys. Chem. Miner.* **1977**, *1*, 385–398.
[61] R. C. Bales, J. J. Morgan, *Geochim. Cosmochim. Acta* **1985**, *49*, 2281–2288.
[62] A. Morgan, P. Davies, J. C. Wagner, G. Berry, A. Holmes, *Br. J. Exp. Pathol.* **1977**, *58*, 465–473.
[63] G. Monchaux, J. Bignon, M. C. Jaurand, J. Lafuma, P. Sebastien, R. Masse, A. Hirsch, J. Goni, *Carcinogenesis* **1981**, *2*, 229–236.
[64] Surface-Chemistry, Structure, and Reactivity of Hazardous Mineral Dust: M. F. Hochella in *Reviews in Mineralogy* (Eds.: G. D. Guthrie, Jr., B. T. Mossman), The Mineralogical Society of America, Washington, DC, USA, **1993**, pp. 275–308.
[65] M. C. Jaurand, L. Magne, J. L. Boulmier, J. Bignon, *Toxicology* **1981**, *21*, 323–342.
[66] M. C. Jaurand, J. Bignon, P. Sebastien, J. Goni, *Environ. Res.* **1977**, *14*, 245–254.
[67] J. Gold, H. Amandusson, A. Krozer, B. Kasemo, T. Ericsson, G. Zanetti, B. Fubini, *Environ. Health Perspect.* **1997**, *105 (Suppl. 5)*, 1021–1030.
[68] M. C. Jaurand, J. Fleury, G. Monchaux, M. Nebut, J. Bignon, *J. Natl. Cancer Inst.* **1987**, *79*, 797–804.
[69] A. Schatz, *J. Agric. Food Chem.* **1963**, *11*, 112–118.
[70] O. W. Purvis, J. A. Elix, J. A. Broomhead, G. C. Jones, *Lichenologist* **1987**, *19*, 193–203.
[71] J. Chen, H. P. Blume, L. Beyer, *Catena* **2000**, *39*, 121–146.
[72] I. B. Beech, J. A. Sunner, K. Hiraoka, *Int. Microbiol.* **2005**, *8*, 157–168.
[73] Z. Elias, O. Poirot, M. C. Daniere, F. Terzetti, A. M. Marande, S. Dzwigaj, H. Pezerat, I. Fenoglio, B. Fubini, *Toxicol. In Vitro* **2000**, *14*, 409–422.
[74] R. Compagnoni, G. Ferraris, L. Fiora, *Am. Mineral.* **1983**, *68*, 214–219.
[75] C. F. Culberson, *Chemical and Botanical Guide to Lichen Products* (Ed.: O. Koelz), University of North Carolina Press, Chapel Hill, **1979**.
[76] F. J. White, P. W. James, *British Lichen Society Bulletin* **1985**, *57 (Suppl.)*, 1–41.

[77] G. R. Buettner, L. W. Oberley, *Biochem. Biophys. Res. Commun.* **1978**, *83*, 69–74.
[78] D. Bersani, P. P. Lottici, A. Montenero, *J. Raman Spectrosc.* **1999**, *30*, 355–360.
[79] H. G. Edwards, M. R. Seaward, S. J. Attwood, S. J. Little, L. F. de Oliveira, M. Tretiach, *Analyst* **2003**, *128*, 1218–1221.
[80] Advanced Industrial Science and Technology, Raman Spectra Database of Minerals and Inorganics (RASMIN), http://www.aist.go.jp/RIODB/rasmin/E_index.htm, **2004**.

Received: July 11, 2006
Published online: February 13, 2007

